Temperature-Sensitive Properties of Poly(*N*-isopropylacrylamide) Mesoglobules Formed in Dilute Aqueous Solutions Heated above Their Demixing Point

Piotr Kujawa,[†] Vladimir Aseyev,[‡] Heikki Tenhu,*[,‡] and Françoise M. Winnik*[,†]

Department of Chemistry and Faculty of Pharmacy, University of Montreal, CP 6128 Succursale Centre Ville, Montreal, QC H3C 3J7, Canada, and Laboratory of Polymer Chemistry, University of Helsinki, PB 55, FIN-00014 HY Helsinki, Finland

Received July 17, 2006; Revised Manuscript Received August 28, 2006

ABSTRACT: The kinetics of merging and/or chain exchange between mesoglobules formed in dilute aqueous solutions of fluorescently labeled poly(*N*-isopropylacrylamides) (PNIPAM) heated above their demixing temperature (T_{dem}) were monitored at specific temperatures between 30 and 50 °C via nonradiative energy transfer (NRET) using polymers carrying ∼0.25 mol % of either naphthyl (Np, energy donor) or pyrene (Py, energy acceptor). Dynamic and static light scattering measurements (DSL and SLS) indicated that PNIPAM-Py and PNIPAM-Np solutions form stable mesoglobules when heated above 30 °C and that the size and size distribution of the mesoglobules depend on solution concentration and, more importantly, on the sample thermal history. Fluorescence depolarization measurements performed on mesoglobular solutions of PNIPAM-Np gave the temperature dependence of the probe anisotropy, an indication of the microviscosity sensed by the probe. The results show that samples heated within the ∼31 °C < T < 36 °C range consist of fluidlike particles able to merge and grow in size. At higher temperatures the mesoglobules act as rigid spheres unable to merge upon collision. These observations are interpreted in terms of the various mechanisms invoked to account for the stability of the PNIPAM mesoglobular phase.

Introduction

When aqueous solutions of thermosensitive polymers are heated to their demixing temperature (T_{dem}), individual chains undergo a collapse from water-swollen coils to compact globules.[1,2] Except in the case of very dilute solutions,[3−5] the globules associate into multichain aggregates, which in many instances stop growing once they attain a certain size. A stable dispersed phase forms consisting of particles, termed mesoglobules, which are monodispersed in size and typically have a radius on the order of 50−200 nm. This phenomenon has been observed e.g. in the case of poly(*N*-isopropylacrylamide) (PNIPAM), poly(*N*-isopropylmethacrylamide), poly(*N*-propylmethacrylamide), poly(*N*-vinylcaprolactam), and poly(vinyl methyl ether).[6−11] Various mechanisms have been proposed to account for the stability of mesoglobules. Pelton et al.,[12] in one of the first articles devoted to the formation of colloidally dispersed phase-separated PNIPAM solutions, suggested that electrostatic repulsion between particles was responsible for the dispersion stability. They demonstrated that the particles were weakly negatively charged and attributed this charge to the presence of some polymer chains with negatively charged end groups introduced by the persulfate salt used to initiate the polymerization of NIPAM. Other researchers, noting that under normal laboratory conditions aqueous solutions always contain traces of low molar mass ions, have suggested that a small number of ions adsorbed on an intrinsically neutral mesoglobule surface may be sufficient to prevent aggregation due to the repulsion between the electric double layers of approaching particles.[13] It has been suggested also that mesoglobules may be sterically stabilized by a shell of dangling chains which remain partly hydrated above T_{dem}, in analogy with the behavior of collapsed amphiphilic polymers for which the hydrophobic backbone folds inside the mesoglobule, while the hydrophilic groups localized at the surface of the globule remain exposed to water.[14,15]

Wu et al. in an investigation of hot aqueous solutions of neutral thermosensitive hydrophobically modified (HM) polymers also observed the occurrence of a mesoglobular phase and suggested that the stability of the mesoglobules was primarily a consequence of the ineffectiveness of the collisions between particles hardened by clusters of hydrophobic substituents acting as cross-linking points.[16] Thus, HM-PNIPAM mesogobules behave as nonadhesive hard spheres for which the contact time upon collision is shorter than the time required to establish permanent chain entanglements between them. From a study of PNIPAM by modulated temperature differential scanning calorimetry (DSC), Van Durme et al.[17] concluded that PNIPAM mesoglobules are partially vitrified; thus, the stabilization mechanism invoking a viscoelastic effect originally proposed for HM-PNIPAM[16] may be effective also in the case of homopolymers. Another factor that contributes to the limited mobility of chains within the PNIPAM mesoglobules is the formation of protein-like intramolecular hydrogen bonds between the carbonyl and the amide groups. These can act as cross-linking points within the globules, slowing down chain motion within the particles.[4,5,18−21]

We report here a photophysical investigation probing the properties of the mesoglobular phase formed upon heating aqueous PNIPAM solutions. We selected this polymer as it is viewed by many as the prototype of the family of hydrosoluble thermosensitive polymers and remains the object of numerous fundamental and applied studies.[22,23] The specific objectives of the study were (i) to obtain a measure of the rigidity ("glassiness") of the mesoglobules and (ii) to assess the effectiveness

[†] University of Montreal.
[‡] University of Helsinki.
* Corresponding author: Ph (514) 340 5179; Fax (514) 340 3245; e-mail francoise.winnik@umontreal.ca.

10.1021/ma061604b CCC: $33.50
Published on Web 10/10/2006

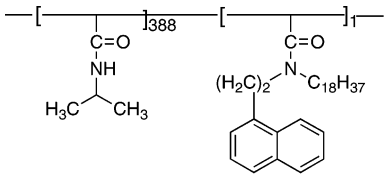

PNIPAM-Np

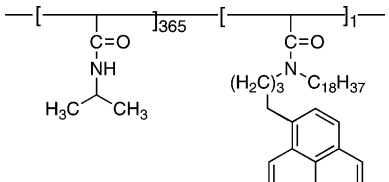

PNIPAM-Py

Figure 1. Chemical structure of the polymers investigated.

of interparticle collisions by following the kinetics of merging of PNIPAM mesoglobules heated to various temperatures beyond T_{dem}. The study was performed with two fluorescently labeled polymers, PNIPAM-Np and PNIPAM-Py (Figure 1), which carry ~0.25 mol % of either a naphthyl-*n*-octadecyl moiety or a pyrenyl-*n*-octadecyl moiety. Fluorescence depolarization measurements were performed on aqueous solutions of PNIPAM-Np in order to determine the temperature dependence of the anisotropy, *r*, of Np, which is an indicator of the rotational freedom of the dye in a given environment and can be related to the microviscosity of the phase in which it is dissolved.[24] Then, we monitored the efficiency of nonradiative energy transfer NRET between Np, the energy donor, and Py, the energy acceptor, in PNIPAM-Np/PNIPAM-Py mesoglobular phases. The efficiency of the NRET process, which originates in dipole/dipole interactions between the two interacting species, decreases rapidly with increasing interchromophore distance.[24] The characteristic distance of the Np/Py pair of chromophore is 29 Å.[25] We followed the time course of the efficiency of NRET immediately upon mixing aqueous solutions of the individual polymers incubated at various temperatures between T_{dem} and 50 °C. These data allowed us to follow the kinetics of interparticle chain exchange and their evolution as a function of temperature. This investigation builds on an early publication by Ringsdorf et al., who exploited the process of NRET between Np and Py in mixed solutions of Np- and Py-labeled hydrophobically modified PNIPAM samples heated and cooled through their demixing temperature (~31 °C).[26] They demonstrated that heating the mixed solutions beyond ~29 °C triggered an increase in the efficiency of energy transfer, which was taken as an indication that, as a result of the contraction of the PNIPAM chains and the subsequent association of collapsed globules, Np and Py find themselves in closer proximity and that their local concentration is higher, compared to the situation in cold water.

Prior to performing the photophysical measurements, we carried out light scattering (LS) and high-sensitivity differential scanning calorimetry (DSC) studies of solutions of PNIPAM-Np and PNIPAM-Py under carefully controlled heating/cooling conditions in order to establish by standard techniques how much the presence of the labels affects the solution properties of PNIPAM and the stability of the mesoglobular phase above T_{dem}. An important conclusion of this investigation is that, in a narrow temperature range in the vicinity of T_{dem}, dilute aqueous PNIPAM-Np or PNIPAM-Py form fluid mesoglobules. In this temperature domain, phase-separated particles merge and grow. Upon further heating, the mesoglobules undergo a conversion from fluid particles to rigid spheres unable to either merge upon collision or undergo chain exchange.

Experimental Section

Materials. Water was deionized with a Millipore Milli-Q system or with an ELGA PURELAB Ultra DV 35. The pyrene- and naphthalene-labeled polymers, PNIPAM-Py and PNIPAM-Np, were obtained by free-radical polymerization as described earlier.[27,28] Their characteristics are given in Table 1.

Table 1. Physical Properties of NIPAM Polymers

polymer	M_n[a]	M_w/M_n[a]	NIPAM:Py or Np[b]
PNIPAM-Py	7.4×10^4	1.7	365:1[27]
PNIPAM-Np	4.9×10^4	1.9	388:1[28]

[a] Number- and weight-average molecular weight (M_n and M_w, respectively) from GPC measurements. [b] Polymer composition from UV−vis spectroscopy.[27,28]

Polymer Characterization. Gel permeation chromatography was performed with a GPC system consisting of an Agilent 1100 isocratic pump, a set of TSK-gel α-M and a TSK-gel α-3000 (Tosoh Biosep) columns, a Dawn EOS multiangle laser light scattering detector (Wyatt Technology Corp.), and an Optilab DSP interferometric refractometer (Wyatt Technology Corp.); injection volume: 100 μL; flow rate: 0.5 mL/min; eluent: DMF; temperature: 40 °C. The d*n*/d*c* value of PNIPAM in DMF at 40 °C was determined to be 0.088 cm^3/g at 690 nm using an Optilab DSP interferometric refractometer (Wyatt Technology Corp). It was assumed that modification of PNIPAM with Np or Py does not influence the d*n*/d*c* value.

Light Scattering Measurements. Dynamic (DLS) and static (SLS) light scattering experiments were performed with a Brookhaven Instrument BIC-200 SM goniometer and BIC-9000 AT digital correlator. An argon ion laser (LEXEL 85, 1 W) operating at a wavelength of 488 nm was used as a light source with power ranging from 10 to 50 mW. In DLS experiments, the autocorrelation functions of the scattered light intensity, $G_2(t)$, were collected at scattering angles, θ, between 30° and 150°. The time average scattered light intensity, I_θ, was recorded simultaneously. The intensities measured in counts of photons per second were normalized with respect to the Rayleigh ratio of toluene. The temperature of the samples was controlled by means of a Lauda RC 6C thermostated water bath. Solutions were passed through Millex-GV/PVDF 0.22 μm filters prior to measurements to remove dust particles. A d*n*/d*c* value of 0.167 mL/g was used to calculate the weight-average molecular weight of samples M_w in water at 20 °C.[29] Solutions for light scattering experiments, ranging in concentration from 0.006 to 0.297 g/L, were prepared from stock solutions (1.0 g/L) kept overnight at 5 °C. Details aspects of the data analysis are reported as Supporting Information.

In the equilibrium (EQ) heating mode, polymer solutions (2.0 mL) were placed in the cell compartment of the light scattering instrument and heated stepwise from 20 to 50 °C in 1−5 °C steps, allowing 2−4 h for equilibration at each temperature. For each temperature setting, the intensity of scattered light (I_θ) was recorded as a function of time. When it reached a constant value, SLS and DLS measurements were performed. The I_θ vs temperature curves were used to determine the cloud point temperature, T_{cp}, defined here as the temperature, at which I_θ starts to increase rapidly upon heating.

In the nonequilibrium (NEQ) heating mode, samples (2.0 mL) were transferred from 5 °C into a water bath preheated to 50 °C (NEQ5 → 50 °C) or 80 °C (NEQ5 → 80 °C). The solutions were kept at 50 or 80 °C in hermetically sealed vials for 24 h. Then, they were cooled by an equilibrium cooling procedure (~0.06 °C/min) from 50 to 36 °C and from 80 to 34 °C. Finally, each solution was reheated to 50 °C at a rate of 0.06 °C/min. These procedures

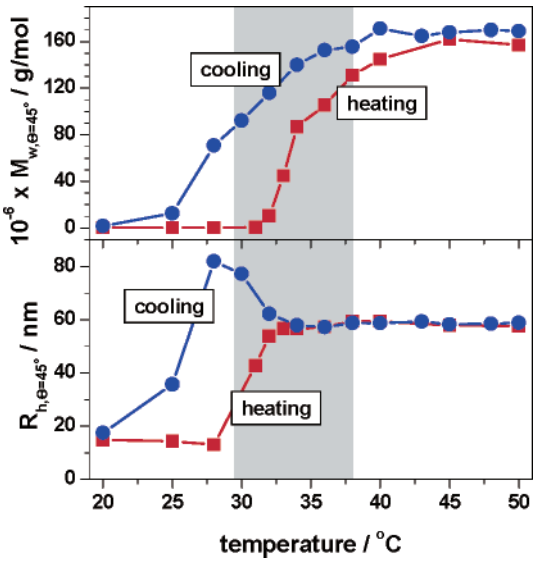

Figure 2. Temperature dependence of the apparent molar mass M_w (a) and the hydrodynamic radius R_h (b) for PNIPAM-Np solutions (polymer concentration: 0.1 g/L; scattering angle: 45°); solutions were heated to 50 °C under equilibrium conditions and cooled at a rate of ≈0.06 deg/min. The shaded area shows the temperature range for mesoglobule formation upon heating.

are referred to as NEQ5 → 50: 50−36−50 °C and NEQ5 → 80: 80−34−50 °C in the text.

Zeta Potential Measurements. Zeta potential measurements were performed with a Nano-ZS Zetasizer (Malvern Instruments) equipped with 4 mW He−Ne laser operating at $\lambda = 633$ nm.

Differential Scanning Calorimetry (DSC). DSC measurements were performed on a VP-DSC microcalorimeter (MicroCal Inc.) at an external pressure of ca. 180 kPa. The cell volume was 0.520 mL. The heating rate varied between 0.16 and 1.5 deg/min. Heating and cooling scans were performed in the temperature range from 10 to 70 °C. Data were corrected for instrument response time to take into account the effect of the scan rate on the data collected. Data were analyzed using the software supplied by the manufacturer. The polymer concentration of the solutions was fixed at 0.1 g/L, the same value as used in fluorescence measurements (vide infra). The temperature of the phase transition (T_M) was taken as the maximum of the transition, the demixing temperature (T_{dem}) was taken as the temperature of onset of the increase in heat capacity (c_p) in a heating scan, and the enthalpy of the transition (ΔH) was determined from the area of the endotherm or exotherm (see Figure 3). At least three measurements were performed for each solution.

Fluorescence Measurements. *Anisotropy Measurements.* Fluorescence anisotropy (r) measurements were performed on a Varian Cary Eclipse spectrometer fitted with two Glan-Thompson polarizers in the L-format configuration. The temperature of the sample fluid was controlled using a water-jacketed cell holder connected to a Cary circulating water bath and measured with a thermocouple immersed in a water-filled cell placed in one of the four cell holders in the sample compartment. The temperature of the sample was changed in a continuous way with a rate of 0.06 deg/min. The slit settings were 5 nm for both excitation and emission. The excitation and emission wavelengths were set at 290 and 330 nm, respectively.

The fluorescence anisotropy was calculated from the relationship

$$r = \frac{I_{VV} - GI_{VH}}{I_{VV} + 2GI_{VH}} \quad (1)$$

where $G = I_{VH}/I_{HH}$ is an instrumental correction factor and I_{VV}, I_{VH}, and I_{HH} refer to the resultant emission intensities at 330 nm polarized in the vertical or horizontal planes (second subindex) upon excitation with either vertically or horizontally polarized light (first subindex). The values reported in the text are the averages of 18 measurements. Solutions for analysis (0.01 g/L) were prepared from an aqueous PNIPAM-Np stock solution (1.0 g/L). Solutions were not degassed prior to measurements.

Nonradiative Energy Transfer Measurements. Steady-state fluorescence spectra were recorded on a Varian Cary Eclipse spectrometer using a water-jacketed cell holder connected to a Cary circulating water bath. The slit settings were 2.5 nm for both excitation and emission monochromators. The emission intensity was monitored at 340 nm (Np) and 376 and 396 nm (Py) with an excitation wavelength of 290 nm. The extent of NRET was taken as the ratio $I_{Py}/I_{Np} = (I_{376} + I_{396})/(2I_{340})$, where I_{376}, I_{396}, and I_{340} are the spectral intensities at 376, 396, and 340 nm, respectively. The ratio was corrected to take into account the contribution to the total emission of the fluorescence of Py excited directly upon irradiation with a 290 nm light, by subtracting $(I_{376} + I_{396})_{PNIPAM-Py}$ from $(I_{376} + I_{396})_{mixed\ solution}$ recorded with solutions of identical PNIPAM-Py concentration (0.025 g/L). The temperature of the sample fluid was measured with a thermocouple immersed in a water-filled cell placed in one of the four cell holders in the sample compartment. The heating or cooling rate was kept at ∼0.06 deg/min, unless stated otherwise. Solutions for fluorescence analysis (concentration: 0.1 g/L) were prepared from aqueous polymer stock solutions (1.0 g/L). The ratio of the Np- to Py-labeled polymers in mixed solutions was [Np]/[Py] = 3/1. This ratio, selected on the basis of spectroscopic considerations, is such that it minimizes direct absorption of light ($\lambda = 290$ nm) by Py and allows efficient NRET from Np* to Py.[28]

The mixing experiments were carried out as follows. In the equilibrium (EQ) heating mode, PNIPAM-Np (0.15 g/L) and PNIPAM-Py (0.05 g/L) solutions were prepared at room temperature, placed in the cell compartment of the spectrofluorimeter, and heated to the measurement temperature at a rate of 0.06 deg/min. They were kept at this temperature for 60 min. After this time, the two solutions were mixed quickly (final polymer concentration: 0.1 g/L; final volume: 4 mL), and the changes with time of I_{Py} and I_{Np} were recorded (kinetic experiments) until the signal remained stable (16−17 h). The solutions were cooled to 18 °C (cooling rate 0.06 deg/min) while monitoring the changes with temperature of I_{Py} and I_{Np}.

In the nonequilibrium (NEQ) mode, solutions of PNIPAM-Np (0.15 g/L) and of PNIPAM-Py (0.05 g/L) placed in hermetically sealed vials were brought quickly from 5 °C to the spectrometer cell holder compartment heated to 50 or 80 °C. They were kept at this temperature for 24 h. They were cooled under equilibrium conditions (0.06 deg/min) to 36 °C. They were mixed at this temperature, and the changes with time of I_{Py} and I_{Np} were recorded (kinetic experiments) until the signal remained stable (16−17 h). These procedures are referred to as NEQ5 → 50: 50−36 °C and NEQ5 → 80: 80−36 °C in the text.

Control experiments performed with solutions of unlabeled PNIPAM (0.1 g/L) indicated that the contribution of scattered light to the total emission intensity was negligible under the high dilution conditions selected, corresponding to ∼0.05% and 0.4% of the total emission intensity for solutions heated below and above T_{dem}, respectively.

Results and Discussion

Aqueous Solutions of PNIPAM-Np and PNIPAM-Py: A Brief Overview. Using light scattering and microcalorimetry, we characterized the solution properties of the fluorescently labeled polymers in cold water and as they undergo the heat-induced phase transition. From a combination of static (SLS) and dynamic light scattering (DLS) measurements, we concluded that PNIPAM-Np in cold water forms small assemblies of monomodal size distribution, consisting of ∼2−3 chains with a hydrodynamic radius (R_h) of ∼14.5 nm. The ratio of the radius of gyration, R_g, over R_h ($R_g/R_h = 1.56$) of the PNIPAM-Np assemblies is characteristic of loose solvent-draining objects,[30] a conclusion confirmed by the low value (0.001 g/cm^3) of ρ, the packing density of polymeric material, defined as the

Table 2. Light Scattering Data for Equilibrium Heated (EQ) Solutions of PNIPAM-Np[a]

conditions	T/°C	M_w/g/mol	A_2/cm^3 mol/g^2	R_g/nm	R_h/nm	R_g/R_h	ρ/g/cm^3
$\theta = 0°$, c = 0.102 g/L	20	$(2.5 \pm 0.1) \times 10^5$	$(-2.2 \pm 0.8) \times 10^{-3}$	22.6 ± 2.1	14.5 ± 0.3	1.56 ± 0.15	0.001 ± 0.001[b]
$\theta = 45°$, c = 0.102 g/L	20	$(2.3 \pm 0.1) \times 10^5$	$(-2.9 \pm 0.8) \times 10^{-3}$	21.1 ± 4.9[c]	14.9 ± 0.3[c]	1.42 ± 0.37	0.001 ± 0.001[b]
	25	$(2.5 \pm 0.1) \times 10^5$	$(-2.3 \pm 0.4) \times 10^{-3}$	21.1 ± 5.9[c]	14.4 ± 0.5[c]	1.46 ± 0.47	0.001 ± 0.001[b]
	28	$(2.4 \pm 0.1) \times 10^5$	$(-3.4 \pm 0.6) \times 10^{-3}$	18.6 ± 4.1[c]	13.0 ± 0.3[c]	1.43 ± 0.35	0.001 ± 0.001[b]
	30	$(3.1 \pm 0.1) \times 10^5$	$(-4.8 \pm 0.5) \times 10^{-3}$	size increases with polymer concentration			
	31	$(4.0 \pm 0.7) \times 10^6$	$(-4.7 \pm 1.5) \times 10^{-4}$	size increases with polymer concentration			
$\theta = 0°$, c = 0.102 g/L[d]	31	$(1.09 \pm 0.01) \times 10^7$	assuming $A_2 = 0$	26.3 ± 4.4	42.0 ± 0.4	0.63 ± 0.11	0.058 ± 0.003[e]
	32	$(4.79 \pm 0.02) \times 10^7$	assuming $A_2 = 0$	35.6 ± 4.3	53.9 ± 0.3	0.66 ± 0.08	0.121 ± 0.002[e]
$\theta = 45°$, c = 0.102 g/L[d]	31	$(1.0 \pm 0.1) \times 10^7$	assuming $A_2 = 0$		42.8 ± 1.0		0.053 ± 0.010[e]
	32	$(4.5 \pm 0.5) \times 10^7$	assuming $A_2 = 0$		53.9 ± 1.0		0.114 ± 0.020[e]
	33	$(8.7 \pm 0.9) \times 10^7$	assuming $A_2 = 0$		56.8 ± 1.0		0.189 ± 0.032[e]
	34	$(1.1 \pm 0.1) \times 10^8$	assuming $A_2 = 0$		56.5 ± 1.0		0.232 ± 0.040[e]
	36	$(1.3 \pm 0.1) \times 10^8$	assuming $A_2 = 0$		57.4 ± 1.0		0.275 ± 0.047[e]
	38	$(1.5 \pm 0.2) \times 10^8$	assuming $A_2 = 0$		59.5 ± 1.0		0.273 ± 0.046[e]
	40	$(1.6 \pm 0.2) \times 10^8$	assuming $A_2 = 0$		59.4 ± 1.0		0.307 ± 0.052[e]
	45	$(1.6 \pm 0.2) \times 10^8$	assuming $A_2 = 0$		57.9 ± 1.0		0.321 ± 0.055[e]
	50	$(1.7 \pm 0.2) \times 10^8$	$A_2 = 0$		57.6 ± 1.0		0.351 ± 0.060[e]
$\theta = 0°$, c = 0.102 g/L	50	$(2.08 \pm 0.03) \times 10^8$	$A_2 = 0$	47.8 ± 5.7	57.8 ± 0.2	0.83 ± 0.10	0.427 ± 0.011[b]

[a] M_w = weight-average molecular weight; A_2 = second virial coefficient; R_g = radius of gyration; R_h = hydrodynamic radius; ρ = density of scatterers. [b] Calculated using the end-to-end distance $h = R_g\sqrt{6}$ as the size of scatterers. [c] There is no concentration dependence of R_g and R_h below T_{cp} within the experimental error; the radii are shown for solution of polymer concentration = 0.102 g/L at $\theta = 0°$. [d] R_g and R_h above T_{cp} increase with increasing polymer concentration that results in apparent value A_2; as demonstrated earlier, the true A_2 ($\approx$0) can be obtained from measurements carried out with solutions obtained by diluting a concentrated solution with hot water.[11] [e] Calculated as for a sphere of radius R_h.

polymer concentration within the volume occupied by a single chain ($\rho = M_w[N_A 4/3\pi R^3]^{-1}$ where R is the end-to-end distance for a coil or R_h for a sphere). Similarly, PNIPAM-Py forms multichain assemblies in cold water with $R_h \sim 18.6$ nm, a value slightly larger than the R_h of PNIPAM-Np, presumably as a consequence of its somewhat larger molecular weight (Table 1). In mixed PNIPAM-Np/PNIPAM-Py solutions associates of intermediate size were detected.

Solutions of PNIPAM-Np (0.006−0.3 g/L) were heated from 20 to 50 °C under equilibrium conditions, following a protocol described in the Experimental Section. The intensity of the scattered light at the angle $\theta = 45°$, $I_{\theta=45}$, remained constant upon heating to 29.5 ± 0.5 °C. It increased rapidly upon further heating and remained constant for $T \geq 38$ °C. The temperature of the onset of the increase in $I_{\theta=45}$ was taken as the cloud point of the solution, T_{cp}. This value is slightly lower than the value typically reported in the literature for dilute solutions of PNIPAM under similar conditions,[22] reflecting the slightly increased hydrophobicity of PNIPAM-Np compared to that of the unmodified polymer. The values of R_h and M_w increase significantly for $T > T_{cp}$ (Figure 2, red curves), indicating the formation of large and dense aggregates, while, concurrently, the second virial coefficient A_2 decreases with increasing temperature due to the worsening of the quality of the solvent in these solutions (Table 2). We noted that the size distribution of the aggregates is monodisperse and that the values of R_h, R_g, and M_w depend significantly on the concentration of the solution (see refs 1 and 11 and Supporting Information, where we present details of the LS study and justify the selection of the methods employed).

Solutions of PNIPAM-Np, equilibrated at 50 °C, were brought back to 20 °C at a rate of ~0.06 deg/min. Values of M_w and R_h recorded upon cooling are plotted in Figure 2 (blue curves). The temperature dependence of M_w in the cooling process follows the trends noted upon heating, except for 27 °C < T < 32 °C, a range of temperature for which M_w values recorded upon cooling are consistently higher than the corresponding M_w values recorded in the heating ramp. Similarly, the R_h values remained constant upon cooling from 50 to ~32 °C. Further cooling triggered an increase of R_h, which reached a maximum value around T_{cp} and decreased sharply within a narrow temperature range to reach eventually the value recorded prior to heat treatment. The hysteresis in the temperature profiles of

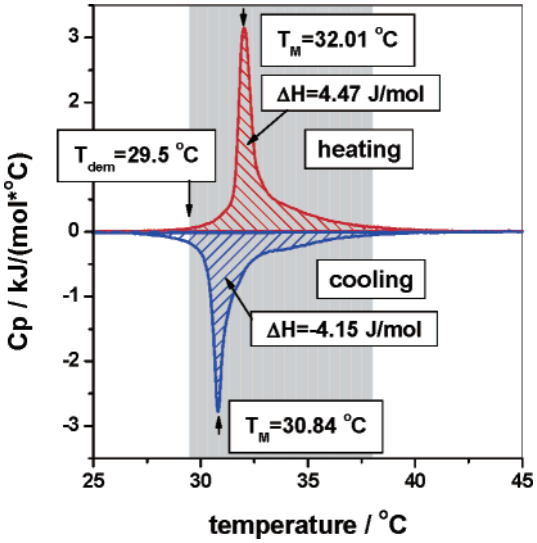

Figure 3. Temperature dependence of the specific heat capacity (c_p) of PNIPAM-Np in water upon heating and cooling at a rate of 0.16 deg/min (polymer concentration: 0.1 g/L). For shaded area, see Figure 2.

R_h corresponding to the formation and to the desintegration of the mesoglobules has been observed also in studies of aqueous PNIPAM solutions.[5,21,31] It was attributed to the fact that in the heating process individual chains undergo intrachain contraction at T_{dem} and subsequent interchain association to form mesoglobules, whereas rehydration upon cooling requires swelling of the globules and breaking of intra- or interchain hydrogen bonds, such that complete unfolding of individual chains occurs when the temperature is lower than the T_{dem}.

The heat-induced phase transition of aqueous PNIPAM-Np solutions was monitored also by microcalorimetry, a technique that yields the changes with temperature of c_p, the partial heat capacity of a solution. In all measurements, the solutions were heated or cooled between 10 and 70 °C, and the heating/cooling rate was adjusted between 0.16 and 1.5 deg/min. Thermograms recorded for an aqueous solution of PNIPAM-Np (0.1 g/L) heated to 70 °C at a rate of 0.16 deg/min and then cooled to 10 °C at the same rate are presented in Figure 3 in which we highlight T_M, the temperature corresponding to the transition maximum, T_{dem}, taken as the temperature of the endotherm onset, and ΔH, the enthalpy of the transition. The T_M and

enthalpy values recorded during the cooling scan are slightly lower than the values observed in the heating process. We observed also that the T_M and ΔH values for solutions of PNIPAM-Np (0.1 g/L) increase with increasing scan rate in the heating ramp, while in the cooling ramp T_M and ΔH decrease slightly upon increasing scan rate (see Supporting Information). Similar trends were noted in previous studies of PNIPAM solutions and gels.[20,32] In the case of PNIPAM-Np and PNIPAM-Py, the values of T_M extrapolated to zero scan rate are 32.05 ± 0.4 and 30.84 ± 0.01 °C for the cooling and heating scans, respectively. The T_{dem} value determined from DSC experiments is ca. 29.5 °C, which coincides with the value obtained by light scattering (vide supra). The fact that the maximum of the exotherm upon cooling occurs at a temperature lower than the endotherm upon heating can be attributed to the fact that intermolecular hydrogen bonds form between PNIPAM chains in collapsed globules, giving them additional stability.[4,5,18−21] Upon cooling, interpolymeric hydrogen bonds are replaced progressively by H-bonds between water molecules and polymer chains. If the cooling process is fast, water molecules have not enough time to penetrate inside the mesoglobules and the reswelling of the mesoglobules is not uniform, leading to a decrease of T_M compared to the value recorded upon heating. Note that the hysteresis observed in the heating/cooling cycle may also be an indication that the PNIPAM mesoglobules are partially vitrified at high temperature and that, consequently, longer equilibration times will be required for remixing to be completed at low temperature.

We measured also the zeta potential, ζ, of mesoglobules formed in aqueous solutions of PNIPAM-Np, PNIPAM-Py, and PNIPAM-Np/PNIPAM-Py 3:1 mixtures (0.1 and 0.03 g/L) heated to 50 °C. In all samples, the ζ value was slightly negative, fluctuating between −9 and −22 mV depending on the heating rate and the polymer concentration (see Supporting Information). These values agree well with those recently published for PNIPAM above its T_{dem}[33] and confirm that the mesoglobules of the labeled PNIPAM samples investigated here also carry a negative surface charge that may, in principle, account for their stability. However, the experimental ζ value is lower than the minimum charge, ∼ −30 mV,[34,35] necessary to provide per se colloidal stability of the mesoglobules. Therefore, even though the electrostatic interactions may contribute to some extent to the stability of mesoglobules, one needs to consider the impact of other mechanisms as well.

In summary, the LS, microcalorimetry, and ζ potential studies provide convincing evidence that although the presence of fluorescent labels on the polymer chains affects somewhat the heat induced phase separation process of PNIPAM, as observed for instance by small shifts in T_{dem} and T_M, the salient features of the mesoglobular phase are preserved. The major impact of the labels is seen in the one-phase systems below the demixing temperature: labeled polymers associate in 2−3 chain associates, whereas PNIPAM chains are isolated from each other, at least in the dilute systems considered here.[22]

Equilibrium Heating/Cooling of Fluorescently Labelled PNIPAM in Aqueous Solutions. *Fluorescence Depolarization Measurements*. A solution of PNIPAM-Np (0.01 g/L), prepared by dilution of a stock solution equilibrated at low temperature, was heated at a constant rate (0.06 deg/h) from 18 to 45 °C. It was kept at this temperature for 14 h and cooled to 18 °C at the same rate. Fluorescence depolarization was measured at fixed temperature intervals, yielding the r values represented in Figure 4 as a function of solution temperature. Note that during the heating scan the anisotropy starts to increase when the solution

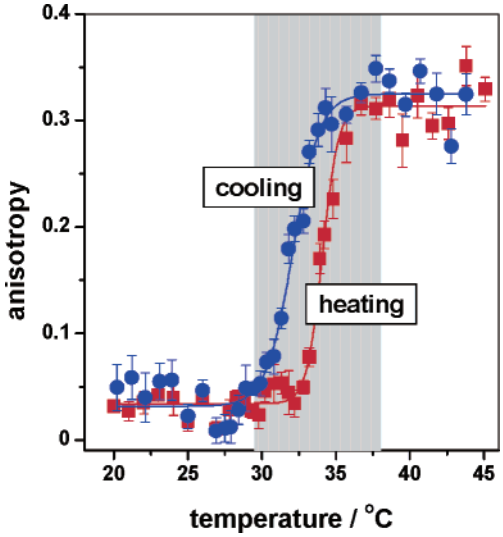

Figure 4. Changes in Np anisotropy as a function of temperature upon heating and cooling for an aqueous solution of PNIPAM-Np (polymer concentration: 0.01 g/L; heating/cooling rate: 0.06 deg/min; λ_{exc}: 290 nm). For shaded area, see Figure 2.

temperature exceeds ∼32.5 °C, a temperature for which mesoglobule formation and growth are nearly completed (see Figure 2). The anisotropy reaches a plateau value for T > 36.5 °C, a temperature beyond which mesoglobule growth stops (Figure 2). Control LS experiments (see Figure S1−2 in Supporting Information) indicate that the difference between the temperature for which changes in anisotropy are first detected and T_{dem} is not due to the fact that fluorescence depolarization experiments were conducted with polymer solutions of concentration higher than the concentration used for LS measurements. The enhancement of r is diagnostic of an increase in the microviscosity sensed by the label, which experiences a rigid "glassy" environment in the mesoglobular phase existing in solutions heated beyond ∼36 °C. The anisotropy temperature profiles recorded upon heating and upon cooling exhibit a hysteresis. The onset of r decrease upon cooling, which signals an increase in probe mobility, takes place when the temperature drops below ∼34 °C, the temperature corresponding to the onset of swelling of the mesoglobules observed by DLS (Figure 2). The decrease of r occurs over a broad temperature range, reaching a constant value for T < 30 °C. Referring again to Figure 2, it appears that the probe has regained its full mobility in water-swollen mesoglobules prior to their full desintegration.

Control frequency-domain fluorescence measurements confirmed that the lifetime of Np* remained constant (50.8 ± 0.6 ns) upon heating the PNIPAM-Np solution from 20 to 45 °C, with no significant changes in its value in the vicinity of the phase transition temperature. The Np* lifetime remained constant during the cooling ramp as well (see Supporting Information). Thus, the temperature-dependent changes in Np anisotropy cannot be due to the difference in the probe lifetime, and they reflect primarily the variation in the microviscosity.

NRET Transfer Measurements. Solutions of PNIPAM-Np and PNIPAM-Py were mixed at 18 °C in amounts such that the total polymer concentration was 0.1 g/L and the [Np]/[Py] ratio was 3/1. The fluorescence of the mixed solution upon excitation at 290 nm, a wavelength of light absorbed selectively by Np, exhibited a contribution of Np* emission in the 310−400 nm range, with a maximum at 340 nm, and an emission between 370 and 500 nm, with maxima at 376 and 396 nm attributed to Py excited via NRET from Np* (Figure 5a). The mixed solution

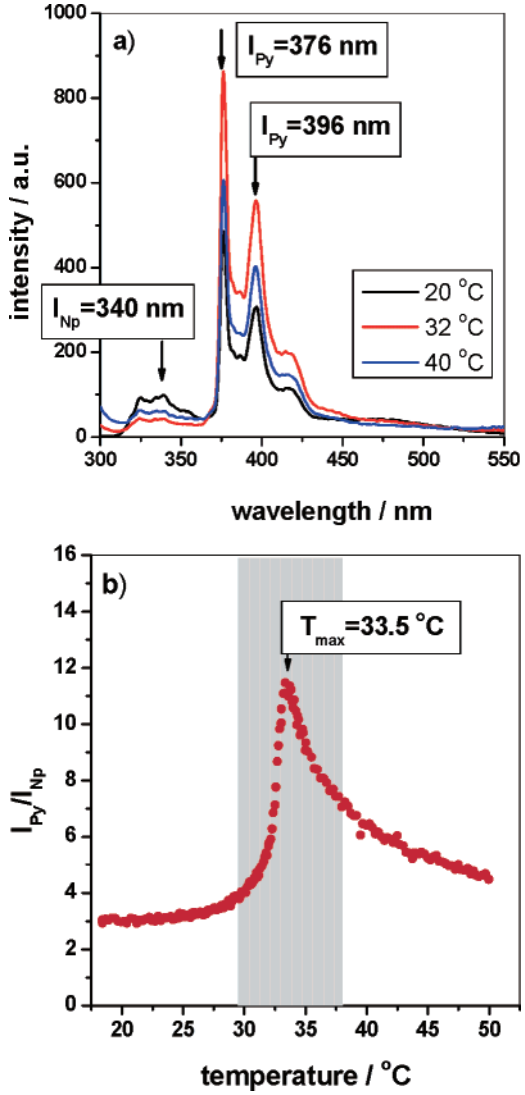

Figure 5. (a) Fluorescence spectra of a solution in water of PNIPAM-Np and PNIPAM-Py recorded at 25, 32, and 40 °C. (b) Changes with temperature of the ratio I_{Py}/I_{Np} of the intensities of the emission of Py and Np for a mixed PNIPAM-Py/PNIPAM-Np solution prepared at 18 °C and subjected to an equilibrium heating treatment. Total polymer concentration: 0.1 g/L, [Np]/[Py] = 3/1; λ_{exc}: 290 nm. For shaded area, see Figure 2.

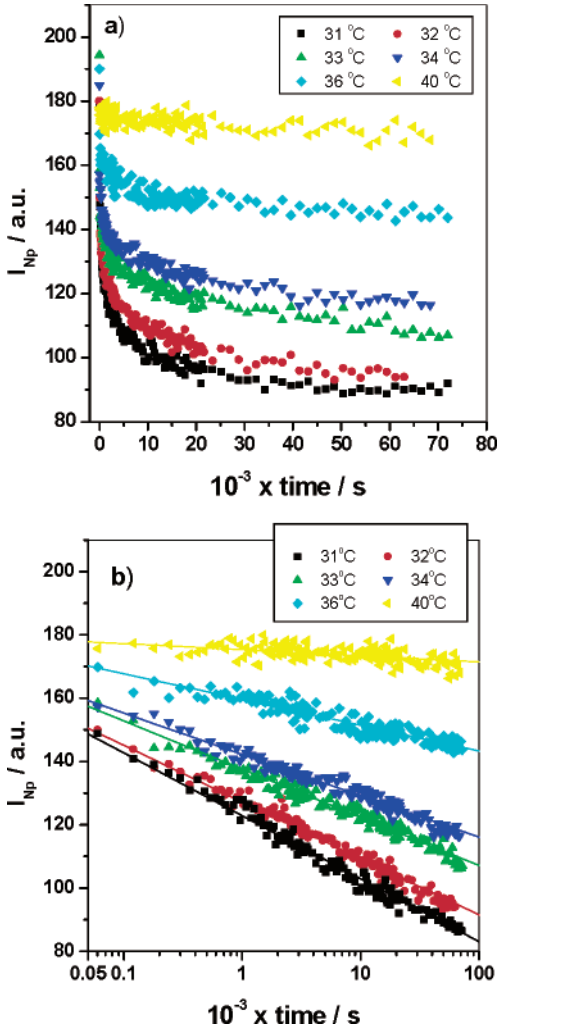

Figure 6. (a) Changes with time of the intensity of Np emission (I_{Np}) following mixing of PNIPAM-Np and PNIPAM-Py solutions incubated at various temperatures in the vicinity of the demixing temperature and higher. Total polymer concentration: 0.1 g/L; [Np]/[Py] = 3/1; λ_{exc}: 290 nm. (b) Data of (a) on a logarithmic time scale. Solid lines display linear fits.

was heated from 20 to 50 °C at a rate of 0.06 deg/min. The Py emission intensity increased with increasing temperature, attained a maximum value as the solution temperature reached 33.5 °C, and decreased upon further heating. Concurrently, the Np emission intensity decreased upon heating, passed through a minimum as the temperature reached 33.5 °C, and increased slightly upon further heating to 40 °C (Figure 5a). The enhancement of the Py emission intensity (I_{Py}) together with the decrease of the Np intensity (I_{Np}) upon heating mixed solutions are diagnostic of the fact that the NRET process becomes more effective with increasing temperature up to 32 °C. Two factors contribute to the effect: (i) the chain dynamics accelerate upon heating, enhancing the probability of chain encounter, and (ii) the probe local concentration increases as a result of solution demixing. The changes with temperature of the efficiency of energy transfer, computed as I_{Py}/I_{Np}, are presented in Figure 5b. In this representation, a high value of I_{Py}/I_{Np} reflects efficient NRET between Np* and Py. In mixed PNIPAM-Py/PNIPAM-Np solutions the conditions for effective NRET seem optimal when the solution temperature is in the vicinity of 33.5 °C, at which point the solution exists in a highly fluid mesoglobular phase (see Figures 2 and 4). The decrease in NRET upon further heating is an indication that at this temperature the microviscosity within the mesoglobule is such that it restricts significantly the segmental motion of the polymer chains, diminishing the frequency of Py/Np encounters.

Next, PNIPAM-Py and PNIPAM-Np solutions were brought to various temperatures between 30 and 40 °C under equilibrium conditions (see Experimental Section). They were rapidly mixed, and the isothermal evolution of the intensity of Np emission was monitored as a function of time. Recall that a decrease in I_{Np} corresponds to an enhancement of the NRET efficiency. Mixing solutions incubated at 31 °C < T < 36 °C, the temperature window for which the mesoglobules are in the fluid regime (see Figures 2 and 4), resulted in a rapid decrease of I_{Np} which slowed down considerably at long times. The amplitude of the change in I_{Np} decreased with increasing incubation temperature (Figure 6a). However, mixing aqueous PNIPAM-Py and PNIPAM-Np samples preheated to T > 36 °C had hardly any effect on the value of I_{Np} recorded for mesoglobular PNIPAM-Np prior to mixing, implying that chain exchange between preformed PNIPAM-Np and PNIPAM-Py mesoglobules and/or mesoglobule merging does not occur under these conditions.

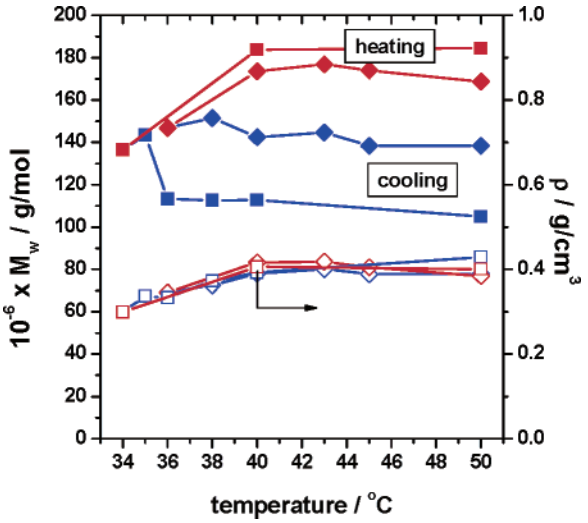

Figure 7. Temperature dependence of the molar mass M_w (full symbols) and the density of the polymeric material within PNIPAM-Np mesoglobules, ρ (open symbols): (squares) solutions heated under nonequilibrium conditions to 80 °C and then subjected to a cooling/heating treatment (NEQ5 → 80: 80−34−50 °C); (diamonds) solutions heated under nonequilibrium conditions to 50 °C and then subjected to a cooling/heating treatment (NEQ5 → 50: 50−36−50 °C); polymer concentration: 0.102 g/L; data obtained at zero scattering angle; the size of the symbols corresponds to the error bars of the values (see Table 2).

We attempted to extract the rate constant of the mixing process from the NRET kinetic data. Poor fits were obtained using single- or double-exponential laws. The data could be fit satisfactorily by a triple-exponential law, but the physical meaning of three finite reaction rates is questionable. We noted though that when the data are plotted on a logarithmic scale ($I_{Np}(t) \sim -\log t$), straight lines are obtained (Figure 6b). Such a time dependence indicates that the systems have no inherent natural mean time constant and that there exists an extremely broad continuous distribution of rate constants that extends over at least 3 decades. One may notice that the equation $I_{Np}(t) \sim -\log t$ implies the existence of a minimum and a maximum cutoff rate constant. However, a careful inspection of Figure 6a indicates that there are no significant deviations at short or long times that would allow an unambiguous determination of these cutoff rates.[36,37]

The slope of the $I_{Np}(t) \sim -\log t$ lines decreases with increasing temperature, implying that, although the distribution function of rate constants remains broad, the average rate constant decreases with temperature (Figure 6b). Similar broad distributions of relaxation times and logarithmic dependence have been reported for systems such as mixing of diblock copolymer micelles,[36] glassy systems,[37,38] protein folding,[39,40] and the internal dynamics of DNA.[41] It is usually ascribed to a broad distribution of activation energies or hierarchical constrained dynamics. In the case of PNIPAM mesoglobules, the broad distribution of relaxation times may be caused by heterogeneities within mesoglobules in terms of chain hydration, conformation, and entanglement.

Nonequilibrium Heating of Fluorescently Labeled PNIPAM Aqueous Solutions. The size and morphology of PNIPAM mesoglobules show a marked dependence on sample history.[6,7,11] In particular, a nonequilibrium heat treatment favors the formation of glassy, or partially vitrified, mesoglobules of smaller size than mesoglobules brought to the same temperature under equilibrium conditions. To ascertain that the same phenomena took place in the case of PNIPAM-Np solutions, we carried out a light scattering study of a PNIPAM-Np solution subjected to a nonequilibrium heat treatment. The sample was heated quickly from 5 °C to 50 or 80 °C and kept at this temperature for 24 h in order to ensure that the system is fully relaxed at this temperature. Subsequently, the sample was cooled to 36 or 34 °C under equilibrium conditions. Full LS characterization of the system was carried out during the cooling process. The mesoglobule properties assessed (R_g, R_h, M_w, and ρ) remained constant upon cooling to ~38 °C. At this point, we noted an increase in M_w (Figure 7, full blue symbols) and a decrease in the mesoglobule density (Figure 7, open blue symbols). These trends indicate that at this temperature the mesoglobules rehydrate and swell. The ratio R_g/R_h decreases below a value of 0.78, characteristic of a molten globule with a denser core.[21] Concurrently, we noted an increase in the size of the mesoglobules, indicating that they undergo effective collisions. To ascertain that mesoglobule growth in this temperature domain does not occur only as a result of swelling, the solutions were heated back to 50 °C and analyzed again by LS (experiments NEQ5 → 80: 80−34−50 °C and NEQ5 → 50: 50−36−50 °C, Figure 7, full red symbols). The particles formed were significantly larger in size and mass than those present at the onset of the experiment. The R_h values recorded for solutions at 50 °C changed from 52.0 nm, prior to cooling, to 55.8 nm, after being cooled to 36 °C and reheated (Table 3). The absence of hysteresis in the particle density (Figure 7, open symbols) confirms that the cooling/heating treatment was performed under equilibrium conditions.

Next, we carried out a series of NRET mixing experiments to assess if the merging of PNIPAM-Np/PNIPAM-Py mesoglobules is affected by the size of the mesoglobules. Thus, solutions of PNIPAM-Py and PNIPAM-Np were heated rapidly from 5 °C to either 50 °C or 80 °C, kept at this temperature for 24 h, and cooled under equilibrium conditions to 36 °C (experiments NEQ5 → 80: 80−36 °C and NEQ5 → 50: 50−36 °C, see Figure 7). The two solutions were then mixed, and the changes in I_{Np} were monitored as a function of time. The results of this experiment are presented in Figure 8 in the form of the time dependence of I_{Np} recorded upon mixing of PNIPAM-Np/PNIPAM-Py solutions brought to 36 °C under equilibrium conditions. The decrease of I_{Np} with time is significantly less pronounced in the case of mesoglobules subjected to the rapid heat treatment, implying that for these samples the chain exchange process is significantly less effective. Also, the exchange is even less pronounced with mesoglobules heated to 80 °C compared to those formed at 50 °C. Mesoglobules that are generated at 80 °C are the smallest among the three samples

Table 3. Light Scattering Data for Equilibrium and Nonequilibrium Heated Solutions of PNIPAM-Np at $T = 50$ °C[a]

conditions	M_w/g/mol	R_g/nm	R_h/nm	R_g/R_h	ρ^b/ g/cm^3
EQ	$(2.08 \pm 0.03) \times 10^8$	47.8 ± 5.7	57.8 ± 0.2	0.83 ± 0.10	0.427 ± 0.01
NEQ5 → 50 °C	$(1.38 \pm 0.02) \times 10^8$	40.1 ± 3.9	52.0 ± 0.3	0.77 ± 0.08	0.389 ± 0.010
NEQ5 → 80 °C	$(1.05 \pm 0.01) \times 10^8$	36.7 ± 2.7	45.9 ± 0.1	0.80 ± 0.06	0.429 ± 0.009
NEQ5 → 80 °C: 80−34−50 °C	$(1.84 \pm 0.03) \times 10^8$	44.6 ± 4.7	56.7 ± 0.2	0.79 ± 0.09	0.401 ± 0.010
NEQ5 → 50 °C: 50−36−50 °C	$(1.69 \pm 0.02) \times 10^8$	43.0 ± 3.4	55.8 ± 0.3	0.77 ± 0.06	0.384 ± 0.010

[a] Polymer concentration: 0.102 g/L (see Experimental Section for the detailed description of the heating/cooling procedure). Molecular weight M_w and hydrodynamic radius R_h were obtained at zero scattering angle ($\theta = 0°$) and zero second virial coefficient $A_2 = 0$. [b] Calculated for a sphere of radius R_h.

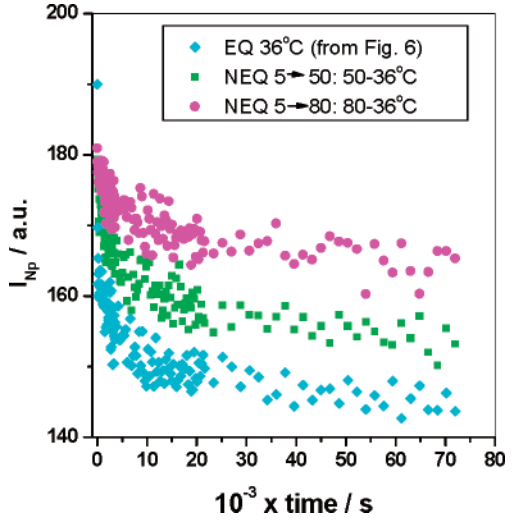

Figure 8. Changes with time of the intensity of Np emission (I_{Np}) following mixing of PNIPAM-Np and PNIPAM-Py solutions at 36 °C: (circles) the solutions were heated separately under nonequilibrium conditions to 80 °C, cooled under equilibrium conditions to 36 °C (NEQ5 → 80: 80−36 °C), and mixed at time 0; (squares) solutions heated separately under nonequilibrium conditions to 50 °C, cooled to 36 °C under equilibrium conditions (NEQ5 → 50: 50−36 °C), and mixed; (diamonds) solutions heated to 36 °C under equilibrium conditions and mixed at 36 °C (data from Figure 6a). Total polymer concentration: 0.1 g/L; [Np]/[Py] = 3/1; λ_{exc}: 290 nm.

tested and, consequently, are expected to diffuse the fastest, but their collisions are the least effective. Their enhanced resistance toward merging can be attributed to an increase in the degree of vitrification of their core in agreement with the conclusions of Van Durme et al.[17]

Conclusions

Fluorescence spectroscopy has allowed us to confirm the contribution of the viscoelastic effect and of the partial PNIPAM vitrification to the mechanism underlying the stability of PNIPAM mesoglobular phases. It also led us to observe directly for the first time that PNIPAM mesoglobules undergo within a narrow temperature window, $T_{dem} < T < 36$ °C, a gradual conversion from fluidlike particles into hard spheres, a phenomenon that had been inferred, but not proven, by light scattering data which indicate that mesoglobules grow in size and mass within this temperature range. The driving force behind this transformation remains unclear. We suggest that changes in the hydration layer surrounding the PNIPAM chains and the exchange of water/polymer H-bonds for interchain H-bonds are involved in the process. Previous studies by FTIR have indicated that mesoglobules heated to ∼40 °C consist of a significant number of water molecules firmly attached to the polymer and that the water molecules loosely bound to the polymer chain below T_{dem} are ejected from the mesoglobules into bulk water in the temperature domain for which our experiments detect enhancement of the mesoglobule rigidity.[18,19,21] Moreover, as suggested by VanDurme et al., for temperatures higher than T_{dem}, vitrification of the mesoglobule core can occur, enhancing particle stability and resistance toward merging.[17] The results of our experiments suggest that this process is significant, but only for $T > 36$ °C, a temperature ∼6−7 °C above T_{dem}. Finally, the possibility that electrostatic effects contribute to the stabilization of PNIPAM mesoglobules cannot be excluded. We are currently conducting experiments in order to elucidate the importance of the latter effect.

Acknowledgment. This work was supported in part by a grant to F.M.W. of the Natural Sciences and Engineering Research Council of Canada. The authors gratefully acknowledge Dr. L. Murtomäki (Helsinki University of Technology) for his help in zeta potential measurements.

Supporting Information Available: Detailed description of the light scattering data analysis including relevant figures, the scan rate dependence of T_M and ΔH obtained from DSC measurements, the fluorescence lifetime data for PNIPAM-Np, and additional data on the zeta potential measurements are provided. This material is available free of charge via the Internet at http://pubs.acs.org.

References and Notes

(1) Aseyev, V.; Tenhu, H.; Winnik, F. M. *Adv. Polym. Sci.* **2006**, *196*, 1−85.
(2) Zhang, G.; Wu, C. *Adv. Polym. Sci.* **2006**, *195*, 101−176.
(3) Wu, C.; Zhou, S. *Macromolecules* **1995**, *28*, 5388−5390.
(4) Wu, C.; Zhou, S. *Phys. Rev. Lett.* **1996**, *77*, 3053−3055.
(5) Wu, C.; Wang, X. *Phys. Rev. Lett.* **1998**, *80*, 4092−4094.
(6) Gorelov, A. V.; Du Chesne, A.; Dawson, K. A. *Physica A* **1997**, *240*, 443−452.
(7) Dawson, K. A.; Gorelov, A. V.; Timoshenko, E. G.; Kuznetsov, Y. A.; Du Chesne, A. *Physica A* **1997**, *244*, 68−80.
(8) Anufrieva, E. V.; Krakovyak, M. G.; Ananieva, T. D.; Lushchik, V. B.; Nekrasova, T. N.; Papukova, K. P.; Sheveleva, T. V. *Polym. Sci. A* **2002**, *44*, 975−979.
(9) Laukkanen, A.; Valtola, L.; Winnik, F. M.; Tenhu, H. *Macromolecules* **2004**, *37*, 2268−2274.
(10) Anufrieva, E. V.; Ananieva, T. D.; Krakovyak, M. G.; Lushchik, V. B.; Nekrasova, T. N.; Smyslov, R. J.; Sheveleva, T. V. *Polym. Sci. A* **2005**, *47*, 189−193.
(11) Aseyev, V.; Hietala, S.; Laukkanen, A.; Nuopponen, M.; Confortini, O.; Du Prez, F. E.; Tenhu, H. *Polymer* **2005**, *46*, 7118−7131.
(12) Chan, K.; Pelton, R.; Zhang, J. *Langmuir* **1999**, *15*, 4018−4020.
(13) Guenoun, P. 231st American Chemical Society Meeting, Symposium on Amphiphilic Polymers, Atlanta, 2006, March 26−30.
(14) Vasilevskaya, V. V.; Khalatur, P. G.; Khokhlov, A. R. *Macromolecules* **2003**, *36*, 10103−10111.
(15) Baulin, V. A.; Zhulina, E. B.; Halperin, A. *J. Chem. Phys.* **2003**, *119*, 10977−10988.
(16) Wu, C.; Li, W.; Zhu, X. X. *Macromolecules* **2004**, *37*, 4989−4992.
(17) Van Durme, K.; Van Assche, G.; Van Mele, B. *Macromolecules* **2004**, *37*, 9596−9605.
(18) Maeda, Y.; Higuchi, T.; Ikeda, I. *Langmuir* **2000**, *16*, 7503−7509.
(19) Maeda, Y.; Higuchi, T.; Ikeda, I. *Langmuir* **2001**, *17*, 7535−7539.
(20) Ding, Y.; Ye, X.; Zhang, G. *Macromolecules* **2005**, *38*, 904−908.
(21) Cheng, H.; Shen, L.; Wu, C. *Macromolecules* **2006**, *39*, 2325−2329.
(22) Schild, H. G. *Prog. Polym. Sci.* **1992**, *17*, 163−249.
(23) Gil, E. S.; Hudson, S. M. *Prog. Polym. Sci.* **2004**, *29*, 1173−1222.
(24) Lakowicz, J. *Principles of Fluorescence Spectroscopy*; Springer: Berlin, 1999.
(25) Winnik, F. M. *Polymer* **1990**, *31*, 2125−2134.
(26) Ringsdorf, H.; Simon, J.; Winnik, F. M. *Macromolecules* **1992**, *25*, 7306−7312.
(27) Ringsdorf, H.; Venzmer, J.; Winnik, F. M. *Macromolecules* **1991**, *24*, 1678−1689.
(28) Ringsdorf, H.; Simon, J.; Winnik, F. M. *Macromolecules* **1992**, *25*, 5353−5361.
(29) Zhou, S.; Fan, S.; Au-Yeung, S. C. F.; Wu, C. *Polymer* **1995**, *36*, 1341−1346.
(30) Burchard, W. *Adv. Polym. Sci.* **1999**, *143*, 113−194.
(31) Wang, X.; Wu, C. *Macromolecules* **1999**, *32*, 4299−4301.
(32) Grinberg, N. V.; Dubovik, A. S.; Grinberg, V. Y.; Kuznetsov, D. V.; Makhaeva, E. E.; Grosberg, A. Y.; Tanaka, T. *Macromolecules* **1999**, *32*, 1471−1475.
(33) Ding, Y.; Ye, X.; Zhang, G. *Macromolecules* **2005**, *38*, 904−908.
(34) Koelmans, H.; Overbeek, J. Th. G. *Discuss. Faraday Soc.* **1954**, *18*, 52−63.
(35) McGown, D. N. L.; Parfitt, G. D. *Discuss. Faraday Soc.* **1966**, *42*, 225−231.
(36) Lund, R.; Willner, L.; Richter, D.; Dormidontova, E. E. *Macromolecules* **2006**, *39*, 4566−4575.
(37) Brey, J. J.; Prados, A. *Phys. Rev. E* **2001**, *63*, 21108.
(38) Tsiok, O. B.; Brazhkin, V. V.; Lyapin, A. G.; Khvostantsev, L. G. *Phys. Rev. Lett.* **1998**, *80*, 999−1002.
(39) Fernandez, A.; Appignanesi, G. *Phys. Rev. Lett.* **1997**, *78*, 2668−2671.
(40) Skorobogatiy, M.; Guo, H.; Zuckermann, M. *J. Chem. Phys.* **1998**, *109*, 2528−2535.
(41) Brauns, E. B.; Madaras, M. L.; Coleman, R. S.; Murphy, C. J.; Berg, M. A. *Phys. Rev. Lett.* **2002**, *88*, 158101.

MA061604B